

DYNAMIC RESPONSE OF FUNCTIONALLY GRADED SHELL-TYPE STRUCTURES TO EXPLOSIVE BLASTS

Terry Hause* and Liviu Librescu**

*Research Engineer, Mankato, MN 56001, USA, **Virginia Tech, Blacksburg, VA 24061, USA

Keywords: *Functionally graded shell; Dynamic response; Shock-wave; Sonic-boom; Explosive blast*

Abstract

The modeling and dynamic response of doubly curved functionally graded panels exposed to explosive type loads considered in conjunction with an uniform through the wall-thickness temperature field are investigated. Two scenarios, symmetric and antisymmetric, continuous distributions of the two constituent phases, ceramic and metal, are considered, in the sense that in one of them the composition varies gradually from ceramic-to-ceramic, while in the other one, from ceramic-to-metal. The implications of the various types of pressure pulses, volume fraction exponent, panel curvature, temperature amplitude, edge load damping ratio, time-history transversal deflection are presented, and pertinent conclusions are drawn.

1 Introduction

During the last few decades there is a sustained effort toward integrating advanced laminated composites in the construction of aerospace and reusable flight vehicle. However, due their well-known shortcoming materialized in terms of delamination and chemical unstable matrix and lamina adhesives, specially at high temperatures, new structural paradigms, enabling one to overcome these adverse effects, have been prompted. The advances in functionally graded materials (FGMs) prompted in [1], that combine the best properties of metals and ceramics, and their applications in various areas of aerospace structures, see e.g. [2,3], can be viewed as an alternative solution for large classes of aerospace structures exposed to se-

vere thermomechanical environments. In this paper, the foundation of the theory of shallow doubly curved shells made from FGMs is presented, and in addition, the problem of their dynamic response to time-dependent loads induced by an explosion, sonic-boom or a shock wave is addressed.

Their effects, considered in conjunction with those induced considered being uniform in space and time will be presented. Pictorial representations of the thickness variation of the two constituent phases, ceramic and metal, are supplied for the two indicated scenarios in Figs. 1a and 1b.

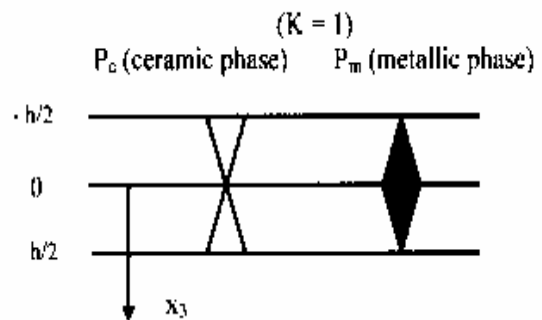


Figure 1a: Thickness distribution of the two phases according to scenario a)

at $x_3 = \pm h/2$, for any k , $V = 1$, and as a result $P(\pm h/2) \Rightarrow P_c$ and for $x_3 = 0$, $V = 0$ and $P(0) \Rightarrow P_m$.

For Case b), the variation of the two phases across the wall thickness is depicted in Fig. 1b. At $x_3 = h/2$, $P(h/2) \Rightarrow P_m$ and for $x_3 = -h/2$, $P(-h/2) \Rightarrow P_c$. At the Midsurface, $x_3 = 0$, and

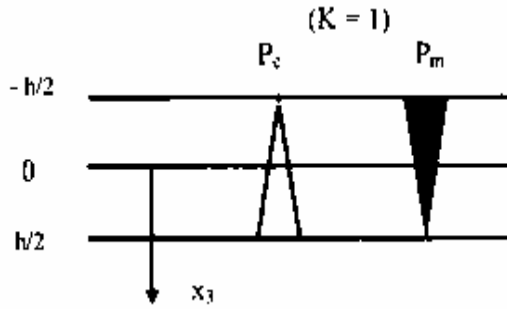


Figure 1b: The counterpart of Fig. 1 for scenario b).

$$\text{for } k=1, P(0) = \frac{1}{2}(P_c + P_m)$$

2 Modeling of the FGM Shell Theory

The points of the shell mid-surface are referred to the Gaussian coordinates x_α , and the thickness coordinate, positive in the downward direction being denoted as x_3 . Based on a simple rule of mixtures, the following form of the variation of mechanical and thermal properties in the (thickness) x_3 direction is postulated as

$$P(x_3) = (P_{\text{ceramic}} - P_{\text{metal}})V(x_3, k) + P_{\text{metal}} \quad (1)$$

where $P(x_3)$ denotes a generic property of the material, in an arbitrary point of the wall structure, P_{ceramic} and P_{metal} are the specific values of the respective properties for the two phases, ceramic and metal, while $V(x_3, k)$ represents the volume fraction of the FGM.

Now, the problem is to express the variation of V according to some pre-determined requirements.

Two scenarios of the grading of the two basic component phases, ceramic and metal, through the wall thickness are considered:

- a) In the case of a high temperature field at both upper and bottom faces of the shell, the phases should vary symmetrically through the wall thickness, in the sense of having full ceramic at the outer surfaces of the shell, and tending toward full metal at its mid-surface, and

- b) In the case of a high temperature at the surface $x_3 = -h/2$, the phases should vary non-symmetrically through the wall thickness, and in this case, there is full ceramic at the outer surface of the shell, and full metal at its inner surface.

In contrast to scenario a) when there is no bending-stretching coupling in the constitutive equations, in the latter one, such coupling exists, and the governing equations become more intricate.

For scenario a), the proper expression of $V(x_3, k)$ is

$$V(x_3, k) = \left(\frac{x_3}{h/2}\right)^k \frac{1 + \text{sgn } x_3}{2} + \left(\frac{x_3}{-h/2}\right)^k \frac{1 - \text{sgn } x_3}{2} \quad (2)$$

where the signum function is given by $\text{sgn}(0) = 0$, -1 for $x_3 < 0$, and $+1$ for $x_3 > 0$; while k , termed the volume fraction index, provides the material variation profile through the wall thickness, ($0 \leq k \leq \infty$).

For scenario b), the composite varies from ceramic to metal, this implying that, the variation of V through the wall thickness should be represented as

$$V(x_3, k) = \left[\frac{h - 2x_3}{2h}\right]^k \quad (3)$$

A proper solution methodology enabling one to determine the structural response due to external loadings that are of an explosive-type will be addressed in this paper. The study will provide also a better understanding of the dynamic response and load carrying capacity of shell-type structures composed of functionally graded materials, with properties varying smoothly and continuously across the structural wall thickness exposed to explosive, shock-wave, and uniform temperature-type loadings.

3 Kinematics and Constitutive Equations

The shell theory considered in this study is a refined one, in the sense of the inclusion of transverse shear effects coupled with those involving consideration of the ceramic-metal FGM materials.

Based on (5a-c), the 3-D strain field is expressed in terms of the 2-D counterpart as

$$\{\varepsilon\} = \{\varepsilon^0\} + x_3 \{\kappa\} \quad (4)$$

where

$$\begin{aligned} \{\varepsilon(x_\alpha, t)\} &= \{\varepsilon_{11}, \varepsilon_{22}, \gamma_{23}, \gamma_{13}, \gamma_{12}\}^T \\ \{\varepsilon^0(x_\alpha, t)\} &= \{u_{0,1} - w_0/R_1, v_{0,2} - w_0/R_2, \\ &w_{0,2} + \psi_2, w_{0,1} + \psi_1, v_{0,1} + u_{0,2}\}^T \\ \{\kappa(x_\alpha, t)\} &= \{\psi_{1,1}, \psi_{2,2}, 0, 0, \psi_{1,2} + \psi_{2,1}\}^T \end{aligned} \quad (5a-c)$$

where γ_{ij} ($i \neq j$) denote the engineering shear strain quantities, and commas denote partial derivatives with respect to the indicated variables.

Using the equations providing the 2-D stress-resultants and stress-moments and assuming for shallow shells that $x_3/R_i \ll 1$, one can get their expressions as

$$\{N\} = [A]\{\varepsilon^0\} + [B]\{\kappa\} - \{N^T\}$$

$$\{N_{\alpha 3}\} = k^2 [A_s]\{\gamma_{\alpha 3}\},$$

$$\{M\} = [B]\{\varepsilon^0\} + [D]\{\kappa\} - \{M^T\}$$

Where,

$$\{N\}^T = \{N_{11}, N_{22}, N_{12}\}, \{N_{\alpha 3}\}^T = \{N_{23}, N_{13}\}$$

and

$$\{M\}^T = \{M_{11}, M_{22}, M_{12}\} \text{ and } k^2$$

is the shear correction factor. (6)

The superscript T denotes transpose operation, while $[A], [A_s], [B]$ and $[D]$ are the stretching,

transverse shear, bending-stretching coupling and bending stiffness matrices, respectively. For FGM, $E = E(x_3)$, $\nu = \nu(x_3)$ and $\alpha = \alpha(x_3)$.

As it clearly appears, these constitutive equations are valid for the non-symmetric distribution of constituent phases across the wall thickness. For the symmetric distribution counterpart, the bending-stretching coupling becomes immaterial, this yielding $[B] = 0$.

4 Governing Equations

Toward getting the governing equations we will use Hamilton's principle formulated as (see e.g.

$$\delta J = \delta \int_{t_0}^{t_1} (U - W - T) dt = 0 \quad (6)$$

where t_0 and t_1 are two arbitrary instants of time, U , W and T denoting the strain energy, the work done by the surface tractions, edge loads and body forces, and the kinetic energy, respectively, while δ the variation operation. As the result of its application from (6) one obtains, consistently with Eq. (5), a tenth order governing systems of partially differential equations, expressed in a compact as,

$$L_{ij} v_j = p_i \quad (i, j = \overline{1,5}) \quad (7)$$

where $L_{ij} = L_{ji}$ are 2-D differential operators, whose expressions are not supplied here.

$v_j = \{u_0, v_0, w_0, \psi_1, \psi_2\}^T$ is the displacement vector, while $p_i(t)$ is the thermomechanical load vector. Consistent with the FSDT (First Order Shear Deformation Theory, the distribution of the 3-D displacement quantities through the wall thickness is postulated as: [3]

$$U_1(x_1, x_2, x_3, t) = u_0(x_1, x_2, t) + x_3 \psi_1(x_1, x_2, t),$$

$$U_2(x_1, x_2, x_3, t) = v_0(x_1, x_2, t) + x_3 \psi_2(x_1, x_2, t),$$

$$U_3(x_1, x_2, x_3, t) = w_0(x_1, x_2, t).$$

(8a-c)

In these equations U_i are the 3-D displacement components along the x_i directions; u_0 , v_0 , and w_0 are the 2-D displacement quantities of the points of the mid-surface, ψ_1 and ψ_2 are the rotations about axes x_2 and x_1 , respectively, and t is the time variable.

$$p_i^T \equiv \left\{ \begin{aligned} &\partial N_{11}^T / \partial x_1, \partial N_{22}^T / \partial x_2, \partial M_{11}^T / \partial x_1, \\ &\partial M_{22}^T / \partial x_2, -N_{11}^T / R_1 - N_{22}^T / R_2 + p_3(t) \end{aligned} \right\} \quad (9)$$

where the superscript T within the brackets identifies the stress-resultant and stress-couples generated by the time-independent temperature field. p_i^T denotes the transpose of p_i while R_1 and R_2 denote the radii of curvature.

4 Thermal Blast Loads

The thermal field ΔT measured from a stress-free reference temperature T_0 is considered to be time and space independent.

Consistent with the Navier Solution to be adopted in the solution of the present boundary-value problem, we represent ΔT as

$$\Delta T = \sum_{m,n=1}^{\infty} T_{mn} \sin \lambda_m x_1 \sin \mu_n x_2$$

which from one obtains that

$$T_{mn} = \frac{4(1-(-1)^m)(1-(-1)^n)}{mn\pi^2} = \quad (10)$$

$$T_{mn} = \frac{16\Delta T}{mn\pi^2} \quad (m,n = 1,3,5\dots).$$

For the thermal stress-results N^T and stress couples M^T associated with the FGM, one can use the same representation as for ΔT , that is

$$N^T = \sum_{n,m=1}^{\infty} N_{mn}^T \sin \lambda_m x_1, \sin \mu_n x_2 \quad (11)$$

$$M^T = \sum_{n,m=1}^{\infty} M_{mn}^T \sin \lambda_m x_1, \sin \mu_n x_2$$

Using the definition of N^T and M^T one gets the expressions of their amplitudes as

$$(N_{mn}^T, M_{mn}^T) = T_1 \int_{-h/2}^{h/2} E(x_3) \alpha(x_3) (1, x_3) dx_3 \quad (12)$$

$$\text{where } T_1 = \frac{16\Delta T}{mn\pi^2(1-\nu)} \quad (m,n=1,3,5\dots).$$

Consistent with the distribution of the material properties in the FGM, one obtains, with Scenario a):

$$N_{mn}^T = T_1 \left[E_{cm} \alpha_{cm} (I_{12}^s + I_{22}^s) + (E_m \alpha_{cm} + E_{cm} \alpha_m) \times (I_{32}^s + I_{42}^s) \right]$$

$$M_{mn}^T = 0 \quad (13a)$$

while for Scenario b):

$$N_{mn}^T = T_1 \left[E_{cm} \alpha_{cm} I_{12}^a + (E_m \alpha_m + E_m \alpha_{cm}) I_{21}^a + E_{cm} \alpha_m h \right]$$

$$M_{mn}^T = T_1 \left[E_{cm} \alpha_{cm} I_{12}^a + (E_m \alpha_m + E_m \alpha_{cm}) I_{22}^a \right] \quad (13b)$$

where, $E_{cm} = E_c - E_m$, $\alpha_{cm} = \alpha_c - \alpha_m$, while the coefficients I_{ij}^s and I_{ij}^a are geometrical quantities associated with the symmetrical or the asymmetrical shells.

As concerns the blast loads, these can be generated by an explosion or by shock-wave disturbances produced by an aircraft flying at supersonic speeds, or by any supersonic projectile, rocket or missile operating in its vicinity.

In the latter case, the blast pulse is referred to as sonic-boom. Its time-history is described as an N -shape pulse, featuring both a positive and a negative phase. Having in view the large blast front generated by the explosion as compared to the relatively small dimensions of the panel, one assumes with sufficient accuracy that the pres-

sure is uniform over the entire panel that is impacted at normal incidence.

The sonic-boom overpressure can be expressed as follows (see e.g. Librescu and Nosier (1990)),

$$p_3(t) = \begin{cases} P_0(1-t/t_p) & \text{for } 0 < t < rt_p \\ 0 & \text{for } t < 0 \text{ and } t > rt_p \end{cases} \quad (14)$$

where P_0 denotes the peak reflected pressure in excess to the ambient one, t_p denotes the positive phase duration of the pulse measured from the time of impact of the structure, and r denotes the shock pulse length factor.

For $r = 1$, the sonic-boom degenerates into a triangular explosive pulse, for $r = 2$, a symmetric sonic-boom pulse is obtained while $r \neq 2$ corresponds to a nonsymmetric N -pulse. When $r = 1$ and $t_p \rightarrow \infty$, in Eq. (14) the N -pulse degenerates in a step pulse.

A more complete expression of the explosive blast pulse as compared to the triangular one is described by the Friedländer exponential decay equation as

$$p_3(t) = P_0 \left(1 - \frac{t}{t_p} \right) e^{-a't/t_p}. \quad (15)$$

where the negative phase of the blast is included. In Eq. (15) a' denotes a decay parameter which has to be adjusted to approximate the pressure curve from the blast test. As it could be inferred, the triangular explosive load may be viewed as a limiting case of Eq. (18), that is for $a'/t_p \rightarrow 0$.

Having in view that Laplace transform method will be used to determine the dynamic response, it is appropriate to express Eq. (16) equivalently (see Marzocca et al. (2001), as

$$p_3(t) = P_0 \left(1 - \frac{t}{t_p} \right) [H(t) - H(t - rt_p)], \quad (16)$$

where $H(t)$ denotes the Heaviside step function. As special cases of Eq. (16), the rectangular and step pressure pulses can be obtained. In the former case

$$p_3(t) = P_0 \{ H(t) - H(t - t_p) \}, \quad (17a)$$

while for the latter one

$$p_3(t) = P_0 \text{ for } \forall t > 0. \quad (17b)$$

The sine pulse that will also be considered in the numerical simulations, is represented as

$$p_3(t) = \begin{cases} P_0 \sin \pi t / t_p & 0 \leq t \leq t_p \\ 0 & t > t_p \end{cases} \quad (18)$$

Finally, in the case of an air-blast traveling in the tangential direction to the panel span, case that will also be considered, the pressure time-history is represented as

$$p_3(t) = P_0 e^{-\eta(ct-x_1)} H(ct - x_1), \quad (19)$$

where c is the wave speed in the medium surrounding the structure, while η is an exponent determining the character of the blast decay.

For a recent study regarding the modeling of gun blast pressure pulses, the reader is referred to Kim and Han (2006).

5 Solution Methodology

An exact solution that can be viewed as an extension of the Navier type solution will be adopted. It corresponds to the case of the simply supported SSI type boundary condition implying that on $x_1 = 0$, L_1 : $v_0 = 0$; $w_0 = 0$; $\psi_2 = 0$; $N_{11} = M_{11} = 0$ and on $x_2 = 0$, l_2 $u_0 = 0$; $w_0 = 0$; $\psi_1 = 0$, $N_{22} = M_{22} = 0$. As is clearly seen,

the SS1-type involves completely moveable edges in the tangential direction.

The solution associated with each displacement unknown is represented as the superposition of two parts a quasi-static and a small dynamic part expressed as

$$V(x_1, x_2, t) = V^s(x_1, x_2) + V^d(x_1, x_2, t) \quad (20)$$

where V denotes a generic displacement quantity.

The boundary conditions are identically fulfilled by expressing the displacement quantities as

$$u_0(x_1, x_2, t) = \sum_{m,n=1}^{\infty} u_{mn}(t) \cos \lambda_m x_1 \sin \mu_n x_2,$$

$$v_0(x_1, x_2, t) = \sum_{m,n=1}^{\infty} v_{mn}(t) \sin \lambda_m x_1 \cos \mu_n x_2,$$

$$\psi_1(x_1, x_2, t) = \sum_{m,n=1}^{\infty} \psi_{1mn}(t) \cos \lambda_m x_1 \sin \mu_n x_2 \quad (21)$$

$$\psi_2(x_1, x_2, t) = \sum_{m,n=1}^{\infty} \psi_{2mn}(t) \sin \lambda_m x_1 \cos \mu_n x_2,$$

$$w_0(x_1, x_2, t) = \sum_{m,n=1}^{\infty} w_{mn}(t) \sin \lambda_m x_1 \sin \mu_n x_2.$$

Consistent with the previous Navier-type representations, we express

$$p_3(t) = \sum_{m,n=1}^{\infty} Q_{mn}(t) \sin \lambda_m x_1 \sin \mu_n x_2$$

where from one gets

$$Q_{mn} = \frac{16}{mn\pi^2} p_3(t) \quad (m, n = 1, 3, 5, \dots) \quad (22)$$

where $p_3(t)$ corresponds to the particular case of blast. Whereas V^s can be determined by using the representation of Eqs. (21) of displacement quantities in the governing equations specialized for the case of zero inertia and a zero transversal load term related with the explosive load. Similarly, V^d can be determined from the governing

equations by keeping the damping and inertia terms as well as the transversal dynamic load term, and discarding in the boundary conditions the thermal terms.

6 Numerical Simulations

The following data for the panel geometry and material properties of constituent material phases are considered in the numerical simulations

Table 1. Material Properties

	Metal (Aluminum)	Ceramic (Alumina)
E , Modulus (GPa)	70	393
ν , Poisson's Ratio (Unitless)	0.3	0.25
ρ , Density (Kg/m ³)	2707	3970
α , Coeff. of Thermal Exp. ($10^{-6}/^{\circ}\text{C}$)	23×10^{-6}	8.8×10^{-6}
C_v , Specific Heat (J/Kg- $^{\circ}\text{C}$)	900	268
kT , Thermal Cond. (W/m-K)	204	10.4
κ , Thermal Diffusivity (m ² /s)	8.373×10^{-5}	9.783×10^{-6}

($L_1 = L_2 = 0.2\text{m}$, $h = 0.004\text{m}$)

References

- [1] Yamanouchi, M., Koizumi, M., Hirai, T., Shiota, I. (Editors) Proceedings of the First International Symposium on Functionally Graded Material, Senday, Japan 1990.
- [2] Librescu, L. and Song, O., *Composite Thin-Walled Beams: Theory and Application*, Springer, 615 pp., 2005.
- [3] Librescu, L., Oh, S-Y. and Song, O., "Thin-Walled Beams Made of Functionally Graded Materials and Operating in a High Temperature Environment: Vibration and Stability," *Journal of Thermal Stresses*, Vol. 28, Nos. 6-7, pp. 649-712, 2005.
- [4] Hause, T., and Librescu, L., "Dynamic Response of Anisotropic Sandwich Flat Panels to Explosive Pressure Pulses," *International Journal of Impact Engineering*, Vol. 31, pp. 607-628, 2005.
- [5] Hause, T., and Librescu, L., "Dynamic Response of Doubly-Curved Anisotropic Sandwich Panels Impacted by Blast Loadings," *International Journal of Solids and Structures*, (in press).
- [6] Librescu, L., Oh, S-Y., and Hohe, J., "Dynamic Response of Anisotropic Sandwich Flat Panels to Underwater and In-Air Explosions," *International Journal of Solids and Structures*, Vol. 43, No. 13, pp. 3794-3816, 2006.

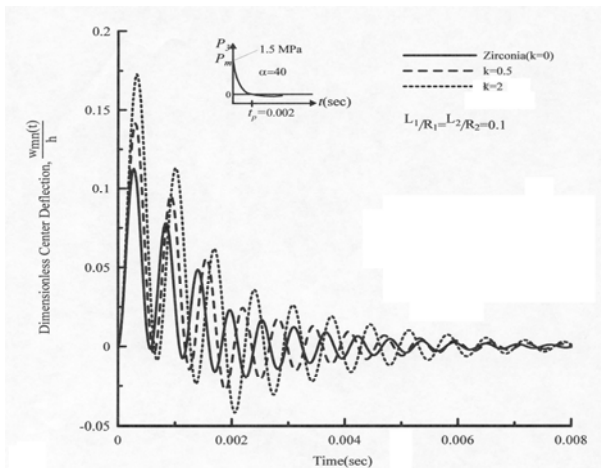


Fig. 1. Center deflection time-history of a FGM spherical cap subjected to an explosive blast, for various values of k .

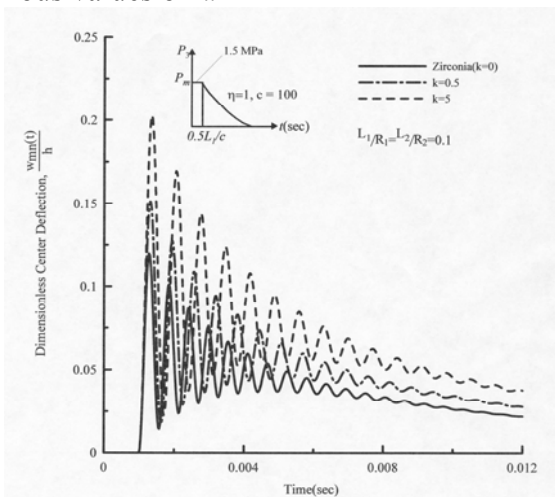


Fig. 2. Counterpart of Fig. 1 for the case of a traveling shock wave.

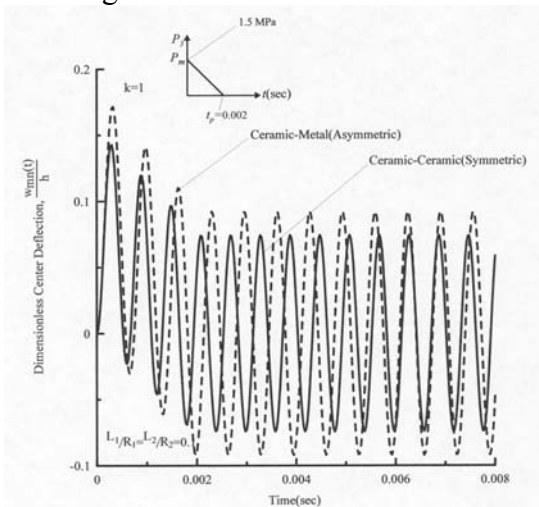


Fig. 3. Effects of the symmetry/asymmetry of phase distribution on the dynamic deflection time-history of a flat panel subjected to a triangular explosive blast.

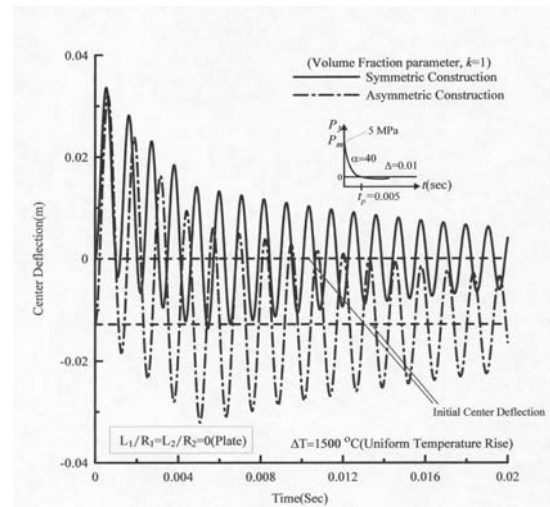


Fig. 4. Effects of the symmetry/asymmetry of phase distribution on the dynamic deflection time-history of a flat panel subjected to an explosive blast and of a uniform temperature ($\Delta T = 1500^\circ\text{C}$).

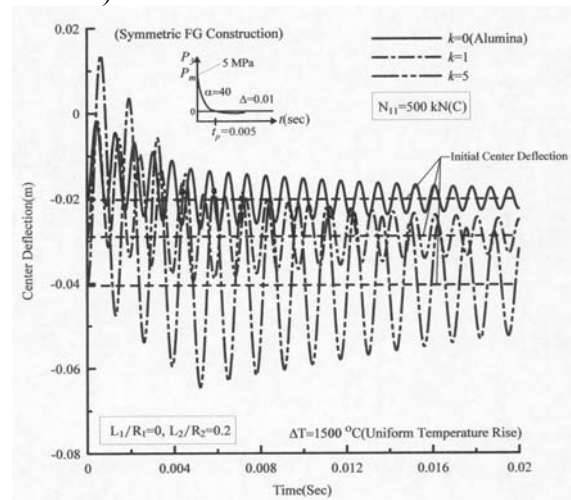


Fig. 5. Effects of the volume fraction exponent on the dynamic response of circular cylindrical panel subjected to an explosive blast, a uniform temperature field ($\Delta T = 1500^\circ\text{C}$) and a compressive edge load.